INTERNATIONAL JOURNAL FOR NUMERICAL METHODS IN FLUIDS
Int. J. Numer. Meth. Fluids 2004; **46**:685–707
Published online 6 September 2004 in Wiley InterScience (www.interscience.wiley.com). DOI: 10.1002/fld.770

2D nearly orthogonal mesh generation

Yaoxin Zhang*,†,‡, Yafei Jia§ and Sam S. Y. Wang¶

National Center for Computational Hydroscience and Engineering, The University of Mississippi, P.O. Box 1500, Oxford, MS 38677, U.S.A.

SUMMARY

The Ryskin and Leal (RL) system is the most widely used mesh generation system for the orthogonal mapping. However, when this system is used in domains with complex geometry, particularly in those with sharp corners and strong curvatures, serious distortion or overlapping of mesh lines may occur and an acceptable solution may not be possible. In the present study, two methods are proposed to generate nearly orthogonal meshes with the smoothness control. In the first method, the original RL system is modified by introducing smoothness control functions, which are formulated through the blending of the conformal mapping and the orthogonal mapping; while in the second method, the RL system is modified by introducing the contribution factors. A hybrid system of both methods is also developed. The proposed methods are illustrated by several test examples. Applications of these methods in a natural river channel are demonstrated. It is shown that the modified RL systems are capable of producing meshes with an adequate balance between the orthogonality and the smoothness for complex computational domains without mesh distortions and overlapping. Copyright © 2004 John Wiley & Sons, Ltd.

KEY WORDS: nearly orthogonal mesh generation; effect-control factor; contribution factor; smoothness control function

1. INTRODUCTION

Computational fluid dynamics (CFD) solves a set of highly non-linear partial differential equations (PDE) in a physical domain, which is usually discretized and represented by a computational mesh. Despite the numerical method used, the success of solving these PDEs depends

*Correspondence to: Y. Zhang, National Center for Computational Hydroscience and Engineering, The University of Mississippi, P.O. Box 1500, Oxford, MS 38677, U.S.A.
†E-mail: yzhang@ncche.olemiss.edu
‡Research Assistant.
§Research Associate Professor and Senior Investigator.
¶F.A.P Barnard Distinguished Professor and Director.

Contract/grant sponsor: USDA Agriculture Research Service; contract/grant number: 58-6408-2-0062
Contract/grant sponsor: The University of Mississippi

Received 14 July 2003
Revised 17 June 2004

largely on the mesh quality. As the general academic criteria, the orthogonality and smoothness are often used to evaluate the mesh quality quantitatively.

Extensive research in the past has made it possible for high quality mesh generation [1–17]. A detailed review of mesh generation research in the 1990s can be found in Reference [18]. One of the most widely used methods for mesh generation was developed by Thompson *et al.* [16] (often referred to as TTM method). In this method, a sophisticated system of Poisson equations with inhomogeneous source terms, called control functions, is solved. The original version of this method cannot generate an orthogonal mapping, unless an appropriate set of control functions is used.

Since the late 1970s, orthogonal mesh generation has been the objective of many researchers [1–12]. The early method for generating 2D orthogonal mesh was through the conformal mapping, but it requires the scale factors be equal in all directions, which somehow punishes the quality of the resulting mesh. Hung and Brown [1] tried to alleviate this problem by using the non-constant, and adjustable distortion function throughout the domain. Mobley and Stewart [3] constructed the orthogonal mapping by using the non-uniform stretching of the conformal co-ordinates. Ryskin and Leal [5] introduced a covariant Laplace equation system for the orthogonal mapping and their success led to the wide use of this system [6–12], often referred to as RL. They identified two kinds of methods corresponding to two kinds of boundaries, namely, 'strong constraint' method and 'weak constraint' method. The former is for domains whose shape is not known in advance, but is to be determined as a part of the solution and the latter is for domains with known prescribed boundary correspondence.

In the RL system, the distortion function f, which is defined as a ratio of the scale factors in two different directions, is no longer constant and needs to be determined. In general, f cannot be prescribed arbitrarily. As classified by Eça [11], there are three different treatments of the distortion function: (1) Calculate f from its definition at the boundaries and then obtain the values in the domain by interpolation or by solving a Laplace equation; (2) specify a class of admissible functions for f to guarantee a unique solution; (3) calculate f from its definition for the whole domain. In order to provide a smooth variation of f throughout the domain, Tamamidis and Assanis [6] used a Laplace equation with a source term to calculate f. Allievi and Calisal [7] calculated f according to its definition in the whole domain and obtained good results, but they claimed their success was due to the Bubnov–Galerkin formulation. Kang and Leal [8] calculated f during the preliminary step in their non-iterative scheme of mesh generation. Duraiswami and Prosperetti [10], based on quasi-conformal mapping theory, specified a class of admissible functions for f. Eça [11] and Akcelik *et al.* [12] also calculated f from its definition in the entire domain during an iteration process.

When using the RL system to generate an orthogonal mapping, in some cases with complex geometries, the local orthogonality constraint may become so restrictive that the local smoothness is sacrificed. This usually results in serious distortion or overlapping of mesh lines in certain region of the domain. In order to prevent mesh lines from overlapping onto each other, Akcelik *et al.* [12] introduced the inhomogeneous source terms into the RL system, which controls favourably the scale factors and hence the aspect ratio of the resulting grid. In Reference [12], a parameter called the force constant is used to optimize mesh empirically.

In this study, two methods are proposed to resolve the mesh distortion and overlapping problems. The first one is an extension of the work of Eça [11] and Akcelik *et al.* [12]

based on the RL system. Compared to Akcelik's work, a set of new control functions for smoothness is introduced into RL system. The control functions are achieved through blending the conformal mapping and the orthogonal mapping. The second method is a novel scheme of the RL system. Contribution factors are introduced to control the grid spaces. A hybrid RL system combining both methods is also proposed. Several examples are discussed in this paper and the comparisons of mesh quality to other methods are demonstrated.

2. MESH GENERATION SYSTEMS

The elliptic system is the most widely used in 2D mesh generation, which is derived from the Laplace equation for the stream function and the velocity potential function. Among these methods, the TTM system developed by Thompson *et al.* [16] and the RL system proposed by Ryskin and Leal [5] are briefly introduced here.

2.1. RL system

Mesh generation is the art of mapping between the physical co-ordinates and the computational co-ordinates. It is assumed that a two-dimensional physical domain is represented by Cartesian co-ordinates $x^i(\equiv x, y),\ i=1,2$ and the corresponding computational domain by generalized co-ordinates $\xi^i(\equiv \xi, \eta),\ i=1,2$ (see Figure 1). Thus the metric tensor g_{ij} can be

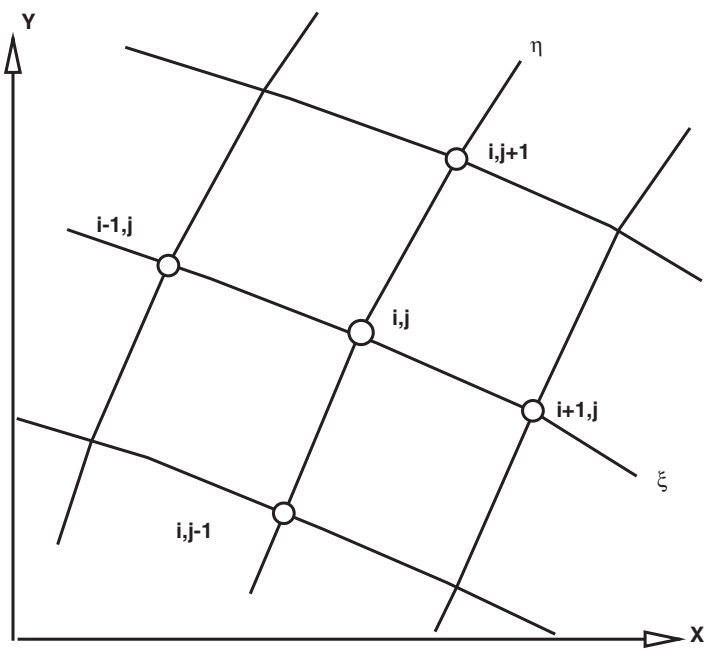

Figure 1. Physical co-ordinate system and computational co-ordinate system.

written as:

$$g = \begin{vmatrix} (x_\xi^2 + y_\xi^2) & (x_\xi x_\eta + y_\xi y_\eta) \\ (x_\xi x_\eta + y_\xi y_\eta) & (x_\eta^2 + y_\eta^2) \end{vmatrix} \tag{1}$$

where $x_\xi = \partial x/\partial \xi$, and so forth.

The simple observation, that the physical co-ordinates satisfy the Laplace equation, can be made. That is,

$$\nabla^2 x^i = 0 \tag{2}$$

A 2D orthogonal mesh must satisfy the condition $g_{12} = g_{21} = 0$, which implies

$$x_\eta = -f \cdot y_\xi \tag{3a}$$

$$y_\eta = f \cdot x_\xi \tag{3b}$$

where the distortion factor f is defined as the ratio of the scale factors in ξ and η direction, i.e.

$$f = \frac{h_\eta}{h_\xi} = \left(\frac{x_\eta^2 + y_\eta^2}{x_\xi^2 + y_\xi^2} \right)^{1/2} \tag{4}$$

and

$$h_\xi = g_{11}^{1/2}, \quad h_\eta = g_{22}^{1/2} \tag{5}$$

If $f = 1$, Equation (3) reduces to the Cauchy–Riemann conditions and the mesh is conformal. According to Equations (2) and (3), the generalized co-ordinates ξ and η satisfy the following partial differential equations:

$$\frac{\partial}{\partial \xi}\left(f \frac{\partial x}{\partial \xi} \right) + \frac{\partial}{\partial \eta}\left(\frac{1}{f} \frac{\partial x}{\partial \eta} \right) = 0 \tag{6a}$$

$$\frac{\partial}{\partial \xi}\left(f \frac{\partial y}{\partial \xi} \right) + \frac{\partial}{\partial \eta}\left(\frac{1}{f} \frac{\partial y}{\partial \eta} \right) = 0 \tag{6b}$$

Equation (6) is the Laplace mesh generation system used by Ryskin and Leal [5].

2.2. *TTM system*

The elliptic system used by Thompson *et al.* [16] for numerical mesh generation is the Poisson equation with the following form:

$$\frac{\partial^2 \xi}{\partial x^2} + \frac{\partial^2 \xi}{\partial y^2} = P(\xi, \eta) \tag{7a}$$

$$\frac{\partial^2 \eta}{\partial x^2} + \frac{\partial^2 \eta}{\partial y^2} = Q(\xi, \eta) \tag{7b}$$

where (ξ, η) is computational co-ordinate system and (x, y) is physical co-ordinate system; P, Q are control functions.

Transforming the above equations, one can obtain,

$$\alpha \frac{\partial^2 x}{\partial \xi^2} - 2\beta \frac{\partial^2 x}{\partial \xi \partial \eta} + \gamma \frac{\partial^2 x}{\partial \eta^2} + \delta \left(P \frac{\partial x}{\partial \xi} + Q \frac{\partial x}{\partial \eta} \right) = 0 \tag{8a}$$

$$\alpha \frac{\partial^2 y}{\partial \xi^2} - 2\beta \frac{\partial^2 y}{\partial \xi \partial \eta} + \gamma \frac{\partial^2 y}{\partial \eta^2} + \delta \left(P \frac{\partial y}{\partial \xi} + Q \frac{\partial y}{\partial \eta} \right) = 0 \tag{8b}$$

where $\alpha = g_{22}$, $\beta = g_{12}$, $\gamma = g_{11}$ and $\delta = g$.

In Reference [16], the control functions were originally constructed to control the grid spacing and clustering effectively, but cannot generate an orthogonal mapping. If the orthogonal condition is applied ($\beta = 0$) and the following control functions are selected, Equation (8) can also generate orthogonal mapping:

$$P = \frac{1}{h_\xi h_\eta} f_\xi, \quad Q = \frac{1}{h_\xi h_\eta} \left(\frac{1}{f} \right)_\eta \tag{9}$$

Substitution of Equation (9) into (8) and rearrangement leads to the RL system.

3. PRESENT STUDY

When the RL system is applied in cases with complex geometries, the local orthogonality constraint may become too restrictive to resolve a good local balance between the orthogonality and the smoothness. Instead, it results in the mesh distortions and overlapping.

Using the central difference scheme to discretize Equation (6) at one typical grid point (i, j), one can obtain:

$$F_{i,j} x_{i,j} = f_{i+1/2,j} x_{i+1,j} + f_{i-1/2,j} x_{i-1,j} + \frac{1}{f_{i,j+1/2}} x_{i,j+1} + \frac{1}{f_{i,j-1/2}} x_{i,j-1} \tag{10a}$$

$$F_{i,j} y_{i,j} = f_{i+1/2,j} y_{i+1,j} + f_{i-1/2,j} y_{i-1,j} + \frac{1}{f_{i,j+1/2}} y_{i,j+1} + \frac{1}{f_{i,j-1/2}} y_{i,j-1} \tag{10b}$$

where

$$F_{i,j} = f_{i+1/2,j} + f_{i-1/2,j} + \frac{1}{f_{i,j+1/2}} + \frac{1}{f_{i,j-1/2}}$$

The generic discretization form can be written as:

$$(x, y)_{i,j} = \sum_{\text{nb}} A_{\text{nb}} (x, y)_{\text{nb}} \tag{11}$$

where 'nb' denotes the neighbouring nodes and A_{nb} is the coefficient.

In regions with mesh distortions and overlapping, the local orthogonal constraint needs to be relaxed. In other words, the location of grid points controlled by the local orthogonal constraint in those regions needs to be adjusted. According to Equation (11), two methods can further alter the location of grid point (i, j). The first method is to add a source term into Equation (11), that is,

$$(x, y)_{i,j} = \sum_{\text{nb}} A_{\text{nb}}(x, y)_{\text{nb}} + S_{i,j} \tag{12}$$

where $S_{i,j}$ is the source term.

This method was first proposed by Akcelik *et al.* [12]. They introduced the inhomogeneous source terms into the RL system to alleviate the above problems. The source terms loosen the local orthogonality somehow to gain more smoothness of the resulting grid. In their method, a parameter called the force constant needs to be adjusted to obtain good results. In the present study, following this idea, a different source term without any parameter is constructed and introduced into the RL system to control the mesh smoothness.

The second method is to modify the coefficient A_{nb}, which is described as

$$(x, y)_{i,j} = \sum_{\text{nb}} A^*_{\text{nb}}(x, y)_{\text{nb}} \tag{13}$$

where A^*_{nb} is the modified new coefficient.

Equation (13) is a novel scheme of the RL system. The modifications to the coefficient A_{nb} should be reasonable to preserve the characteristics of the RL system.

A combination of these two methods can also be easily obtained:

$$(x, y)_{i,j} = \sum_{\text{nb}} A^*_{\text{nb}}(x, y)_{\text{nb}} + S_{i,j} \tag{14}$$

3.1. Method 1: smoothness control functions

In Equation (8), β, P and Q play important roles for orthogonal mesh generation. The cross-derivative term β is a measure of deviation from full orthogonality, which has been assumed zero. The source terms P and Q control the clustering of interior nodes for orthogonality, which can be considered as the measures of local deviation from smoothness. If it is too strong to maintain the local balance between the orthogonality and the smoothness, the local orthogonality constraint should be relaxed by reducing the effects of local P and Q. Based on this point of view, an *effect-control factor* is introduced into Equation (8).

$$\alpha\frac{\partial^2 x}{\partial\xi^2} - 2\beta\frac{\partial^2 x}{\partial\xi\partial\eta} + \gamma\frac{\partial^2 x}{\partial\eta^2} + \delta\left[(1 - r_P)P\frac{\partial x}{\partial\xi} + (1 - r_Q)Q\frac{\partial x}{\partial\eta}\right] = 0 \tag{15a}$$

$$\alpha\frac{\partial^2 y}{\partial\xi^2} - 2\beta\frac{\partial^2 y}{\partial\xi\partial\eta} + \gamma\frac{\partial^2 y}{\partial\eta^2} + \delta\left[(1 - r_P)P\frac{\partial y}{\partial\xi} + (1 - r_Q)Q\frac{\partial y}{\partial\eta}\right] = 0 \tag{15b}$$

where $r_P(\in[0, 1])$ and $r_Q(\in[0, 1])$ are *effect-control* factors in the ξ and η directions, respectively.

Comparison of Equations (8) and (15) shows that the effect-factors r_P and r_Q have the effect of blending the conformal mapping and the orthogonal mapping. When they are equal

to 1, Equation (15) is reduced to the Laplace equation for the conformal mapping; and when they are equal to 0, Equation (15) turns to the Poisson equation for the orthogonal mapping.

Substitution of the orthogonal condition and Equation (9) into Equation (15) leads to the following equations:

$$\frac{\partial}{\partial\xi}\left(f\frac{\partial x}{\partial\xi}\right)+\frac{\partial}{\partial\eta}\left(\frac{1}{f}\frac{\partial x}{\partial\eta}\right)+P_x+Q_x=0 \tag{16a}$$

$$\frac{\partial}{\partial\xi}\left(f\frac{\partial y}{\partial\xi}\right)+\frac{\partial}{\partial\eta}\left(\frac{1}{f}\frac{\partial y}{\partial\eta}\right)+P_y+Q_y=0 \tag{16b}$$

Equations (16a) and (16b) are to be compared with Equations (6a) and (6b). The additional terms P_x, Q_x, P_y and Q_y are called smoothness control functions. According to the connection between the RL system and the TTM system, they are derived as the following forms:

$$(P_x,P_y)=-r_P f_\xi\frac{\partial(x,y)}{\partial\xi} \tag{16c}$$

$$(Q_x,Q_y)=-r_Q\left(\frac{1}{f}\right)_\eta\frac{\partial(x,y)}{\partial\eta} \tag{16d}$$

The *effect-control* factors r_P and r_Q can be either constants or variables over the domain. If they are constant for the whole domain, every grid point will be evenly posed as a blended effect of a conformal mapping and an orthogonal mapping. For those grids that already have a good balance of smoothness and orthogonality, this blending is unnecessary and may even have negative affects. Thus, to reach the best balance of smoothness and orthogonality for the whole domain, the effect-control factors should be spatially varied. In this study, the following empirical formulas are constructed to evaluate the effect control factors.

$$r_P=\frac{|\bar{h}_\xi-h_\xi|}{\bar{h}_\xi} \tag{17a}$$

$$r_Q=\frac{|\bar{h}_\eta-h_\eta|}{\bar{h}_\eta} \tag{17b}$$

where $\bar{h}_\xi$ and $\bar{h}_\eta$ are the locally averaged scale factors in the ξ and η directions, respectively, and for the grid point (i,j), they are defined by

$$\bar{h}_\xi=\frac{(h_\xi)_{i+1,j}+(h_\xi)_{i-1,j}}{2} \tag{17c}$$

$$\bar{h}_\eta=\frac{(h_\eta)_{i,j+1}+(h_\eta)_{i,j-1}}{2} \tag{17d}$$

In Equation (17), the difference between the local scale factor and the local averaged scale factor is considered as a measure of deviation from smoothness. When the difference is zero, a good balance of smoothness and orthogonality is assumed and no adjustment is needed. With the difference increasing, the effect-control factor increases and the adjustment for smoothness also increases in order to reach the balance. In this way, the global balance of smoothness and orthogonaly can be reached.

One can obtain the first modified RL system in discretized form as follows:

$$F_{i,j}x_{i,j} = f_{i+1/2,j}x_{i+1,j} + f_{i-1/2,j}x_{i-1,j} + \frac{1}{f_{i,j+1/2}}x_{i,j+1} + \frac{1}{f_{i,j-1/2}}x_{i,j-1} + (P_x)_{i,j} + (Q_x)_{i,j} \tag{18a}$$

$$F_{i,j}y_{i,j} = f_{i+1/2,j}y_{i+1,j} + f_{i-1/2,j}y_{i-1,j} + \frac{1}{f_{i,j+1/2}}y_{i,j+1} + \frac{1}{f_{i,j-1/2}}y_{i,j-1} + (P_y)_{i,j} + (Q_y)_{i,j} \tag{18b}$$

where

$$F_{i,j} = f_{i+1/2,j} + f_{i-1/2,j} + \frac{1}{f_{i,j+1/2}} + \frac{1}{f_{i,j-1/2}}$$

Equations (16a) and (16b) have the same forms as those of Reference [12]. Compared with the pure empirical source terms with an undetermined parameter in Reference [12], Equations (16c) and (16d) are derived from the blended conformal mapping and orthogonal mapping, which makes the source terms introduced into the RL system within a reasonable range.

3.2. *Method 2: contribution factors*

In Equation (10), it is observed that the movement of any interior node depends on the contributions from its four neighbouring nodes and it tends to move toward the neighbour with more contribution. If the local distortion function f of its neighbour is extremely high, grid point (i, j) would move closer to this neighbour, causing a higher value of the distortion function f. In other words, the growth of the distortion function is not bounded so that it could result in more serious mesh distortion and overlapping.

To avoid this problem, a contribution factor is introduced into Equation (10).

$$F_{i,j}x_{i,j} = f_{i+1/2,j}c_{i+1,j}x_{i+1,j} + f_{i-1/2,j}c_{i-1,j}x_{i-1,j} + \frac{c_{i,j+1}}{f_{i,j+1/2}}x_{i,j+1} + \frac{c_{i,j-1}}{f_{i,j-1/2}}x_{i,j-1} \tag{19a}$$

$$F_{i,j}y_{i,j} = f_{i+1/2,j}c_{i+1,j}y_{i+1,j} + f_{i-1/2,j}c_{i-1,j}y_{i-1,j} + \frac{c_{i,j+1}}{f_{i,j+1/2}}y_{i,j+1} + \frac{c_{i,j-1}}{f_{i,j-1/2}}y_{i,j-1} \tag{19b}$$

where $F_{i,j} = f_{i+1/2,j}c_{i+1,j} + f_{i-1/2,j}c_{i-1,j} + c_{i,j+1}/f_{i,j+1/2} + c_{i,j-1}/f_{i,j-1/2}$ and $c_{i,j}$ is the contribution factor of grid point (i,j) defined as follows:

$$c_{i+1,j} = (d_{i+1,j})^{\alpha} = \left(\sqrt{(x_{i,j} - x_{i+1,j})^2 + (y_{i,j} - y_{i+1,j})^2}\right)^{\alpha} \tag{20a}$$

$$c_{i-1,j} = (d_{i-1,j})^{\alpha} = \left(\sqrt{(x_{i,j} - x_{i-1,j})^2 + (y_{i,j} - y_{i-1,j})^2}\right)^{\alpha} \tag{20b}$$

$$c_{i,j+1} = (d_{i,j+1})^{\alpha} = \left(\sqrt{(x_{i,j} - x_{i,j+1})^2 + (y_{i,j} - y_{i,j+1})^2}\right)^{\alpha} \tag{20c}$$

$$c_{i,j-1} = (d_{i,j-1})^{\alpha} = \left(\sqrt{(x_{i,j} - x_{i,j-1})^2 + (y_{i,j} - y_{i,j-1})^2}\right)^{\alpha} \tag{20d}$$

where $d_{i+1,j}$ is the distance between point (i,j) and point $(i+1,j)$ and $\alpha \in [0,1]$ is a parameter.

As shown in Equations (19) and (20), the contribution factor is evaluated by the distance of the grid point (i,j) and its neighbours. The neighbour with longer distance has larger contribution factor, while the neighbour with smaller distance has smaller contribution factor. Therefore, for one grid point (i,j), if the distortion function f of one neighbour is high, which implies that the distance between them is small, then the contribution factor of that neighbour is also small, which will decrease the contribution of that node. This mechanism can confine the vicious cycle and thus make the mesh smoother.

Note that the exponential parameter α is in the range of 0 and 1. When $\alpha \to 0$, Equation (19) approaches to Equation (10), the original RL system. In Equation (6), the distortion function f is usually calculated strictly from its definition to ensure a unique solution. Equation (19) adjusts the distortion function locally using the contribution factor, such adjustment, however, should be limited to avoid the divergence of the solution.

3.3. Hybrid method

An immediate extension of the above two methods leads to a hybrid RL system as follows:

$$F_{i,j}x_{i,j} = f_{i+1/2,j}c_{i+1,j}x_{i+1,j} + f_{i-1/2,j}c_{i-1,j}x_{i-1,j} + \frac{c_{i,j+1}}{f_{i,j+1/2}}x_{i,j+1} + \frac{c_{i,j-1}}{f_{i,j-1/2}}x_{i,j-1} + [(P_x)_{i,j} + (Q_x)_{i,j}] \cdot r_C \tag{21a}$$

$$F_{i,j}y_{i,j} = f_{i+1/2,j}c_{i+1,j}y_{i+1,j} + f_{i-1/2,j}c_{i-1,j}y_{i-1,j} + \frac{c_{i,j+1}}{f_{i,j+1/2}}y_{i,j+1} + \frac{c_{i,j-1}}{f_{i,j-1/2}}y_{i,j-1} + [(P_y)_{i,j} + (Q_y)_{i,j}] \cdot r_C \tag{21b}$$

where c, P_x, Q_x, P_y and Q_y are defined in Equations (20) and (16); $r_C \in [0,1]$ controls the effects of the smoothness control functions.

With the exponential parameter $\alpha = 0$ and $r_C = 0$, Equation (21) will be reduced to Equation (10) (original RL); with $\alpha = 0$ and $r_C = 1$, Equation (18) (RL with smoothness control functions) will be obtained; and with $\alpha > 0$ and $r_C = 0$, Equation (21) will turn to Equation (19) (RL with contribution factors).

4. SOLUTION PROCESS

The numerical procedure of Equation (21) is an iterative process similar to that of Reference [10]. The maximum difference between the grid co-ordinates in consecutive steps is used as the convergence condition.

$$\max\left(\sqrt{(x_{i,j}^n - x_{i,j}^{n-1})^2 + (y_{i,j}^n - y_{i,j}^{n-1})^2}\right) < 10^{-6} \tag{22}$$

where n is the iteration number.

The linear Equation (21) is solved iteratively and the iterative algorithm is as follows:

a. Identify the boundaries of the domain and use an algebraic method to obtain an initial mesh.
b. Calculate the distortion function f from its definition Equation (4).
c. Calculate the smoothness control functions from Equation (16).
d. Calculate the contribution factors from Equation (20).
e. Solve Equation (21) with fixed f obtained from step b, the smoothness control functions from step c and the contribution factors from step d.
f. Update the mesh and check if the convergence condition is satisfied. If not, repeat steps from b to f.

5. BOUNDARY CONDITIONS

The mesh generation based on the elliptic system is a boundary value problem, and the boundary conditions have significant influences on the resulting mesh.

Either the Dirichlet or the Neumann boundary conditions can be applied to solve the elliptic system. As stated in Reference [14], Equations (6) and (8) are second-order PDEs, which can support only one set of boundary conditions. That is, the Dirichlet and the Neumann boundary conditions cannot be enforced simultaneously.

The Dirichlet boundary conditions are generally used to solve the elliptic mesh generation system. If the Neumann conditions are applied, the Dirichlet conditions must be dropped, which may make the resulting mesh not boundary-fitted. To resolve this problem, a kind of Dirichlet–Neumann conditions is usually used to simulate the Neumann boundary conditions

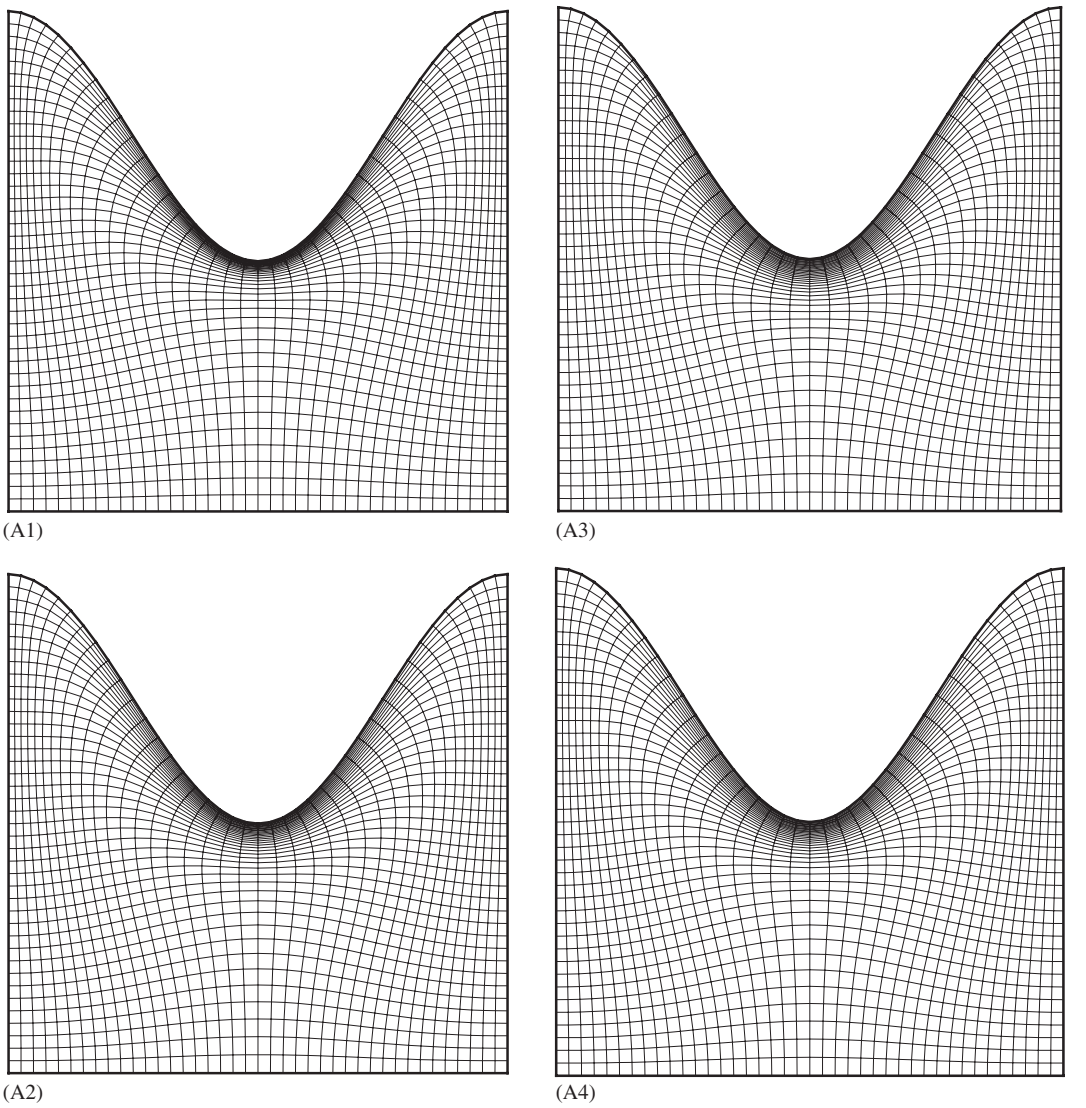

Figure 2. Meshes in domain A with the Dirichlet conditions in all boundaries: (A1) the RL system; (A2) the RL with smoothness control functions; (A3) the RL with contribution factors, $\alpha = 0.01$; and (A4) the hybrid RL system, $\alpha = 0.005$ and $r_C = 0.5$.

[11]. That is, the grid points slide along the boundary (Dirichlet) to satisfy the Neumann conditions.

In the present study, the Dirichlet conditions are used for all the boundaries and the Dirichlet–Neumann conditions (sliding boundary conditions) will also be explored to test the effects of the boundary conditions on the mesh quality.

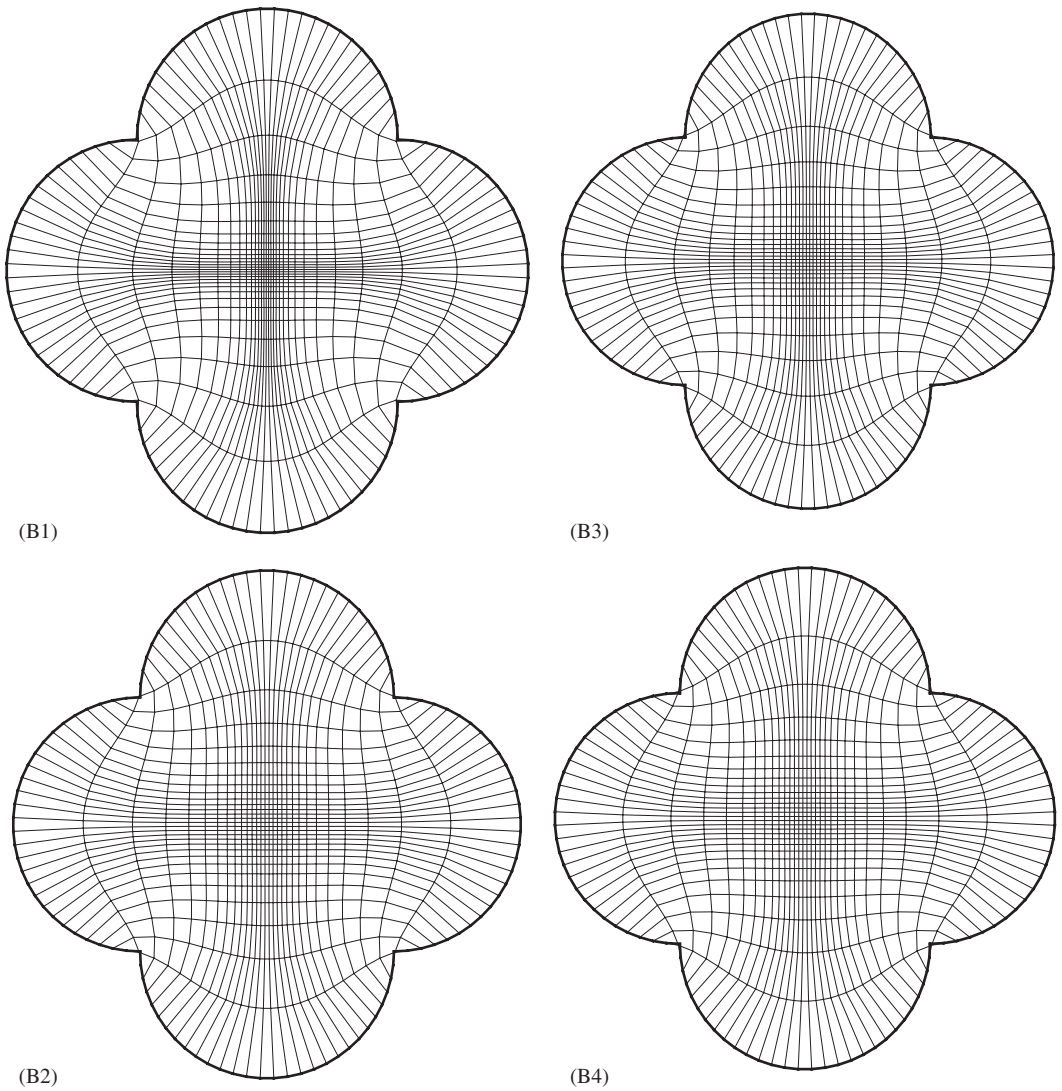

Figure 3. Meshes in domain B with the Dirichlet conditions in all boundaries: (B1) the RL system; (B2) the RL with smoothness control functions; (B3) the RL with contribution factors, $\alpha = 0.01$; and (B4) the hybrid RL system, $\alpha = 0.002$ and $r_C = 0.5$.

6. EXAMPLES AND DISCUSSIONS

Several cases commonly used in the literatures [7–12] are selected as examples here for illustration and discussion. Although the adaptivity, referring to the control of the mesh density distribution according to the physics of a particular problem, is often used to evaluate the mesh quality, in this paper the quality of mesh is evaluated quantitatively by several indicators, such

Table I. Evaluation of meshes in domains A and B.

Domain	Case	Size	ADO	MDO	AAR	MAR	α	r_C
A	A1	41×41	0.07	0.62	4.86	33.9	0	0
	A2	41×41	0.16	0.92	3.84	18.9	0	0
	A3	41×41	0.15	0.72	3.57	13.7	0.01	0
	A4	41×41	0.14	0.82	3.70	16.1	0.005	0.5
B	B1	30×30	0.07	4.28	4.22	13.0	0	0
	B2	30×30	0.33	9.57	2.70	7.5	0	0
	B3	30×30	0.19	8.0	3.31	9.4	0.01	0
	B4	30×30	0.23	7.89	2.96	8.3	0.002	0.5

as maximum deviation orthogonality (MDO), averaged deviation from orthogonality (ADO), maximum grid aspect ratio (MAR), and averaged grid aspect ratio (AAR).

The MDO and ADO, which are used to evaluate the orthogonality of a mesh, are defined as

$$\mathrm{MDO} = \max(\theta_{i,j}) \tag{23a}$$

$$\mathrm{ADO} = \frac{1}{(ni-2)}\frac{1}{(nj-2)}\sum_{2}^{ni-1}\sum_{2}^{nj-1}\max(\theta_{i,j}) \tag{23b}$$

where ni and nj are the maximum number of mesh lines in ξ and η directions, respectively; and θ is defined as

$$\theta_{i,j} = \arccos\left(\frac{g_{12}}{h_\xi h_\eta}\right)_{i,j} \tag{24}$$

The MAR and AAR, which are used to evaluate the smoothness of a mesh, are defined as

$$\mathrm{MAR} = \max\left[\max\left(f_{i,j}, \frac{1}{f_{i,j}}\right)\right] \tag{25a}$$

$$\mathrm{AAR} = \frac{1}{(ni-2)}\frac{1}{(nj-2)}\sum_{2}^{ni-1}\sum_{2}^{nj-1}\max\left[\max\left(f_{i,j}, \frac{1}{f_{i,j}}\right)\right] \tag{25b}$$

6.1. Symmetric domains

The following symmetric domains are selected to compare the proposed methods and the original RL system:

(1) Domain A (with concave boundary) is bounded by $x=0$, $x=1$, $y=0$, and $y=0.75+0.25\sin(\pi(0.5+2x))$.
(2) Domain B is a unit square with one half-circle on each side.

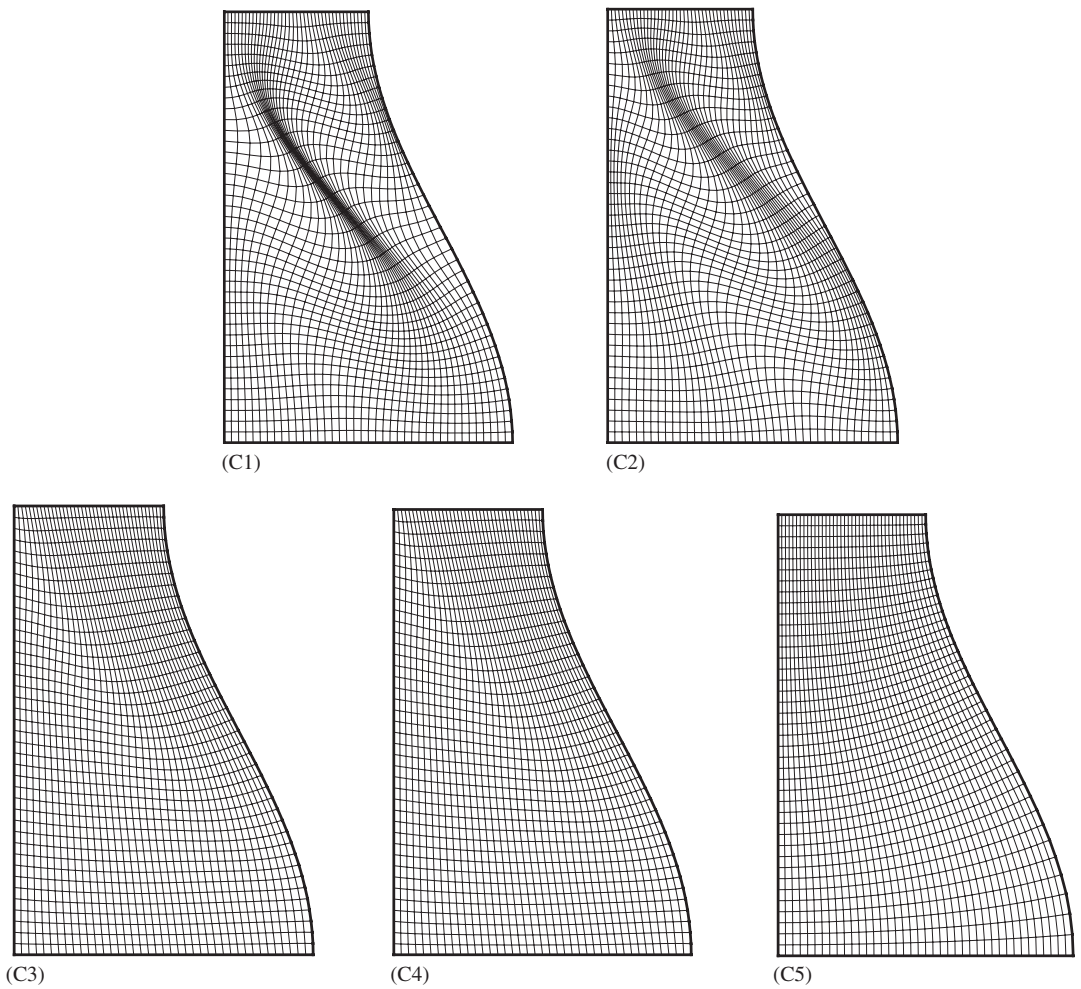

Figure 4. Meshes in domain C: (C1) the RL system, the Dirichlet conditions in all boundaries; (C2) the RL with smoothness control functions, the Dirichlet conditions in all boundaries; (C3) the RL with contribution factors, $\alpha = 0.2$, the Dirichlet conditions in all boundaries; (C4) the hybrid RL system, $\alpha = 0.2$ and $r_C = 1.0$, with the Dirichlet conditions in all boundaries; and (C5) the RL system, the sliding conditions for the right curved boundary and the Drichlet conditions in other boundaries.

Initial meshes with uniform nodal distribution along the four boundaries, namely, top boundary, bottom boundary, left boundary, and right boundary, were generated by the algebraic method. Figures 2 and 3 show the comparisons of meshes with different methods for domains A and B, respectively. Table I summarizes the quality of meshes.

The mesh lines are contracted to the concaved top boundary in domain A, and to the centre lines of domain B in x and y directions. The original RL system generated the best orthogonal meshes with the worst smoothness. Using the modified RL systems, the smoothness of the

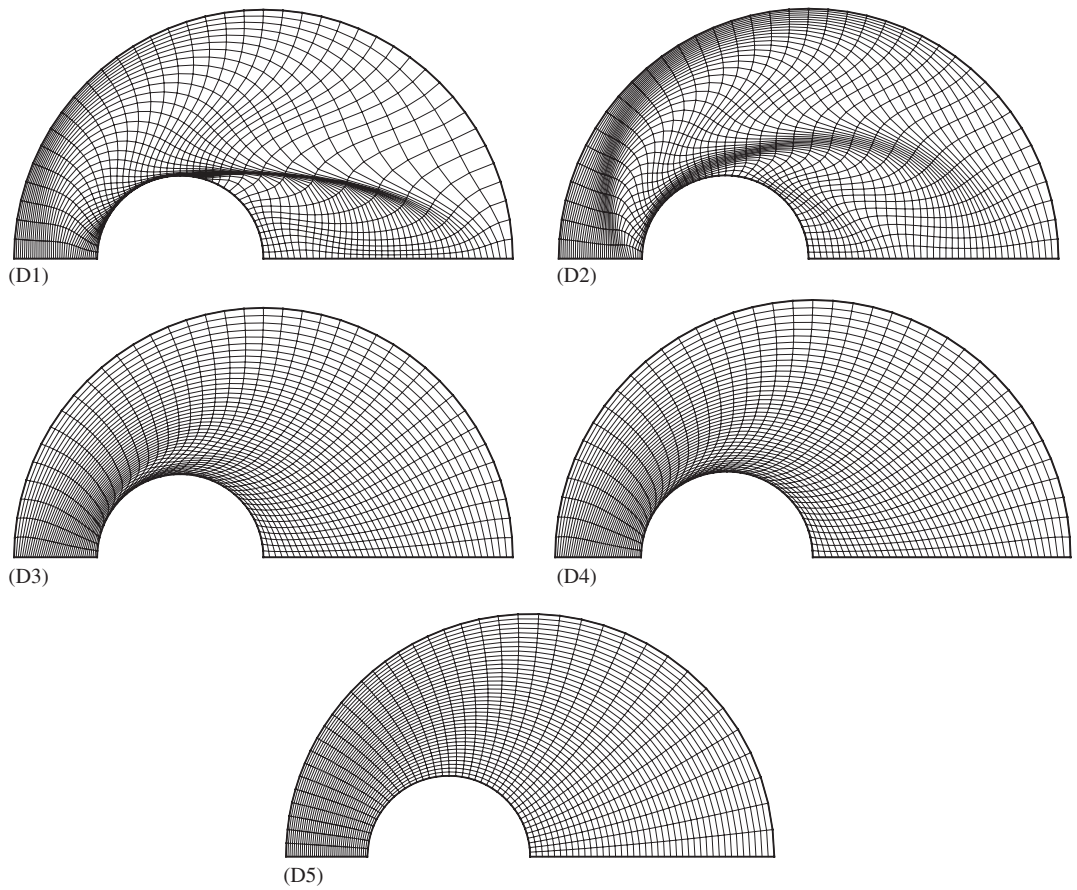

Figure 5. Meshes in domain D: (D1) the RL system, the Dirichlet conditions in all boundaries; (D2) the RL with smoothness control functions, the Dirichlet conditions in all boundaries; (D3) the RL with contribution factors, $\alpha = 0.6$, the Dirichlet conditions in all boundaries; (D4) the hybrid RL system, $\alpha = 0.5$ and $r_C = 1.0$, with the Dirichlet conditions in all boundaries; and (D5) the RL system, the sliding conditions for the two circles and the Drichlet conditions in other boundaries.

resulting mesh has been improved significantly with the orthogonality suppressed a little. The smoothest mesh was obtained from the RL system with contribution factors, and the hybrid RL system produced better mesh in smoothness than the RL system with smoothness control functions.

6.2. *Asymmetric domains*

Two asymmetric domains are used to further test the proposed methods.

(1) Domain C is bounded by $x = 0$, $y = 0$, $y = 1$, and $x = \frac{1}{2} + \frac{1}{6}\cos(\pi y)$.
(2) Domain D is bounded by two-half circles and x-axis. The radius of the small circle is one-third of that of the big one.

Table II. Evaluation of meshes in domains C and D.

Domain	Case	Size	ADO	MDO	AAR	MAR	α	r_C
C	C1	41×41	0.37	1.11	3.98	46.1	0.0	0.0
	C2	41×41	0.65	1.41	2.88	12.4	0.0	0.0
	C3	41×41	1.98	3.42	2.25	3.75	0.2	0.0
	C4	41×41	2.02	3.28	2.25	3.76	0.2	1.0
	C5	41×41	0.02	0.07	2.21	2.99	0.0	0.0
D	D1	41×41	0.62	3.70	147.00	5373.00	0.0	0.0
	D2	41×41	1.32	5.1	5.24	17.2	0.0	0.0
	D3	41×41	3.22	13.2	3.06	8.36	0.6	0.0
	D4	41×41	4.24	13.9	3.04	8.40	0.5	1.0
	D5	41×41	0.04	0.13	3.55	6.80	0.0	0.0

In these two domains, equidistant nodal distribution along all the boundaries was also used for the initial algebraic meshes. The resulting meshes are displayed in Figures 4 and 5, and the mesh quality is reported in Table II.

The Dirichlet conditions were applied in all boundaries for cases C1–C4 and D1–D4. Using the original RL system, serious mesh distortions and overlapping occurred within both domains. Using the RL with smoothness control functions, the smoothness was not improved sufficiently and the mesh distortions still exist. Only the RL with contribution factors and the hybrid RL removed the mesh distortions and overlapping at a little cost of the orthogonality.

Using the original RL system, the applications of the sliding boundary conditions to the right-curved boundary of domain C and to the two circles of domain D successfully resolved the mesh distortions and overlapping. The overall mesh quality was improved greatly due to the sliding boundary conditions. It is shown that in these asymmetric domains, the original RL system is sensitive to the nodal distributions along the boundaries.

6.3. Sensitivity analysis

Domain C is also used to study the effects of the initial meshes on the modified RL systems. The resulting mesh of case C1 with the mesh distortions and overlapping is used as the initial mesh for the modified RL systems. Figure 6 shows the resulting meshes and Table III summarizes the mesh quality. It is found that the modified RL systems are not sensitive to the initial conditions. Little difference can be identified between cases 6–8 and their counterpart cases 2–4.

A symmetric domain E with concave boundary (similar to domain A but with smaller curvature) bounded by $x = 0$, $x = 1$, $y = 0$, and $y = 0.8 + 0.2\cos(2\pi x)$ is used to study the relationships between the exponential parameter α and those academic criteria (ADO, MDO, AAR and MAR) (Table IV).

The resulting meshes using different values of α are shown in Figure 7. Figure 8 shows the ADO, MDO, AAR and MAR as the functions of α. Not surprisingly, with α increasing, ADO and MDO increase, and AAR and MAR decrease. When α approaches to 1, the AAR still decreases, but the MAR begins to increase. This is the reason that α should be bounded

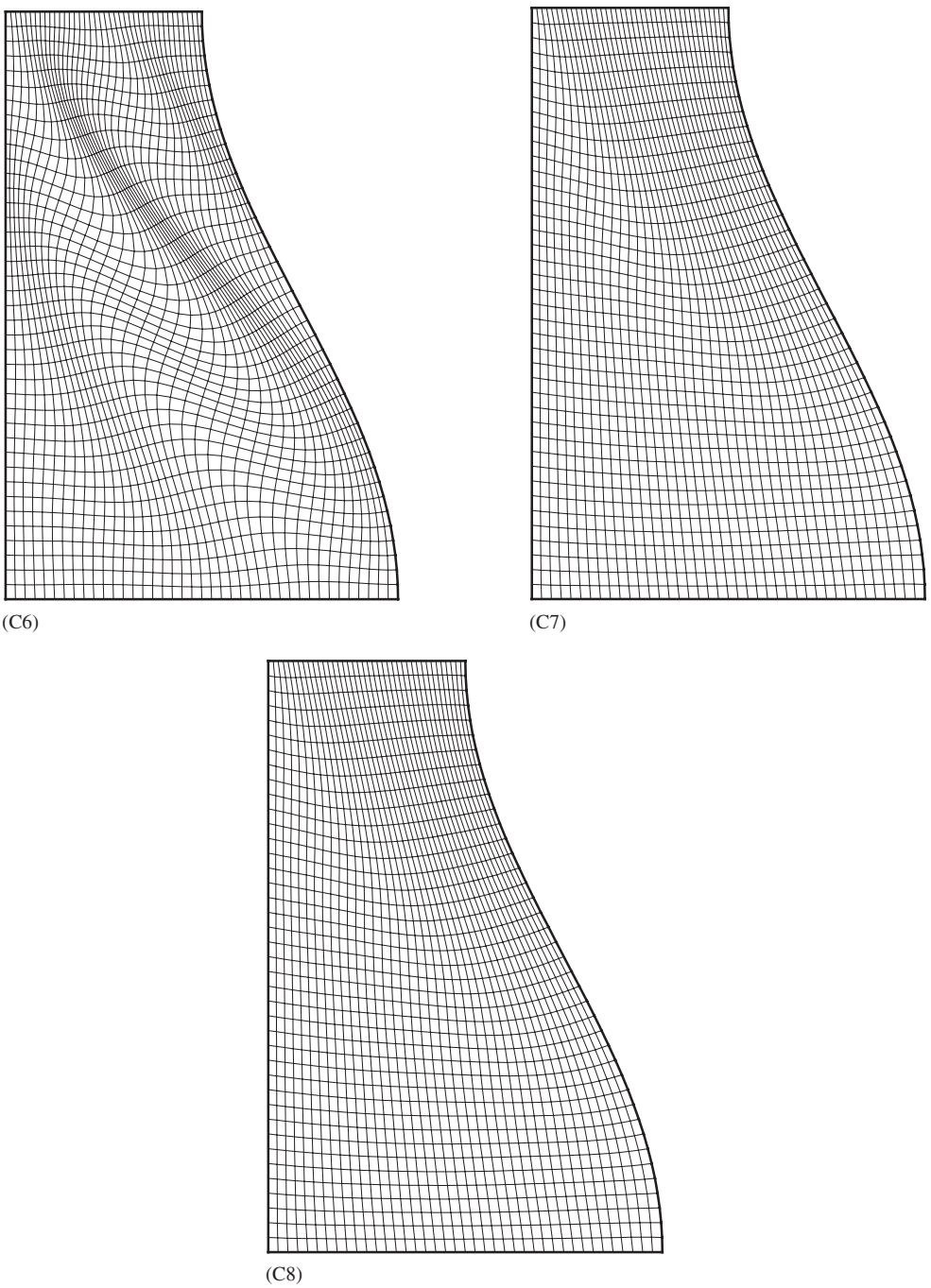

Figure 6. Sensitivity analysis of initial conditions in domain C using the resulting mesh of case (C1): (C6) the RL with smoothness control functions; (C7) the RL with contribution factors, $\alpha = 0.2$; and (C8) the hybrid RL system, $\alpha = 0.2$ and $r_C = 1.0$.

Table III. Evaluation of meshes in domains C.

Domain	Case	Size	ADO	MDO	AAR	MAR	α	r_C
C	C6	41×41	0.78	1.53	2.72	9.55	0	0
	C7	41×41	1.99	3.33	2.25	3.78	0.20	0
	C8	41×41	2.04	3.24	2.24	3.75	0.20	1.0

Table IV. Evaluation of meshes in domain E.

Domain	Case	Size	ADO	MDO	AAR	MAR	α	r_C
E	E1	41×41	0.06	0.26	1.79	6.47	0.01	0
	E2	41×41	0.48	1.25	1.66	5.17	0.10	0
	E3	41×41	1.15	2.89	1.52	4.73	0.30	0
	E4	41×41	1.86	4.76	1.40	4.46	0.70	0

within the range of 0 and 1. Figure 9 shows the effect of α on the iteration steps. A little increase of α can reduce the number of iteration significantly.

7. APPLICATION

In order to test the robustness of the proposed methods, a natural river channel (domain F) is selected. The original RL system is compared to the modified RL system with smoothness control function, the modified RL system with contribution factors and the hybrid RL system. The channel boundaries are irregular and there were two hydraulic structures built in this reach, which made it difficult for mesh generation.

The initial mesh was created by the algebraic method and the nodal distribution along the boundaries was non-uniform. The Dirichlet boundary conditions were used for all boundaries. Figure 10 shows the resulting meshes and Table V summarizes the evaluation of mesh quality.

In this natural river with irregular boundaries, it is difficult to apply the sliding boundary conditions. The original RL system failed to generate an acceptable mesh without mesh distortion and overlapping, while the modified RL systems improved the smoothness greatly. The best smooth mesh still comes from the RL with the contribution factors.

8. CONCLUSIONS

The RL is one of the most widely used generation system for the orthogonal mapping. Using the RL system practically, a strictly orthogonal mesh may neither be possible nor useful in cases with complex geometries. On the contrary, a nearly orthogonal mesh with a good balance between the orthogonality and the smoothness is often preferred. In the present study, two methods for balancing the mesh orthogonality and smoothness are proposed. The first one is a modified RL system with the smoothness control functions, which are constructed through blending the conformal mapping and the orthogonal mapping. The second method is

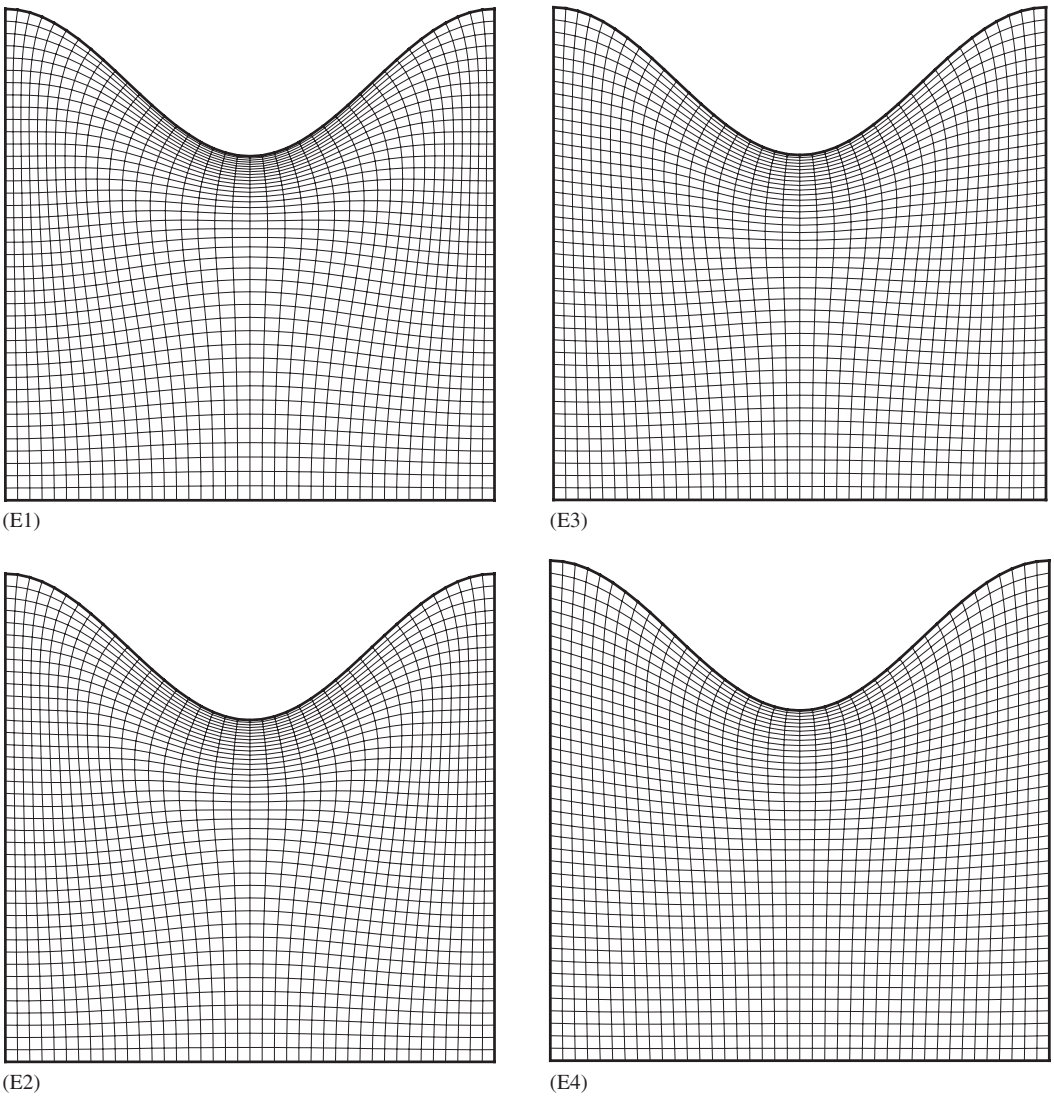

Figure 7. Meshes in domain E with the Dirichlet conditions in all boundaries: (E1) RL with contribution factors, $\alpha = 0.01$; (E2) RL with contribution factors, $\alpha = 0.1$; (E3) RL with contribution factors, $\alpha = 0.3$; and (E4) RL with contribution factors, $\alpha = 0.7$.

a modified RL system with the contribution factors. A hybrid RL system combining these two methods is also developed. Comparisons between the RL system and the modified RL systems have been illustrated by several examples and application.

In the first modified RL system, the *effect-control* factor is constructed to automatically adjust the balance between the orthogonality and the smoothness for the whole domain. With the effect-control factor increasing, the local smoothness increases and the local orthogonality

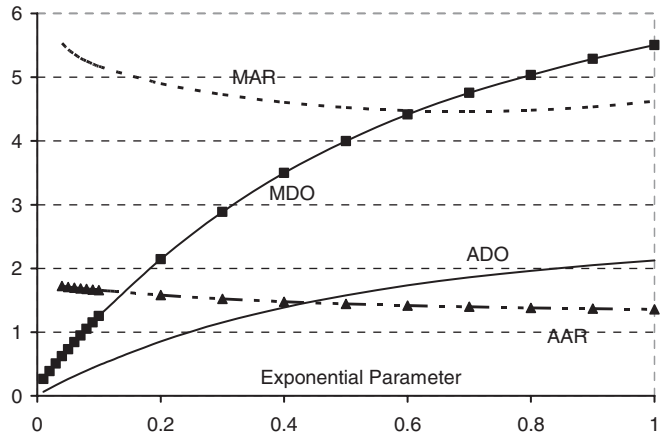

Figure 8. Effect of exponential parameter on mesh quality.

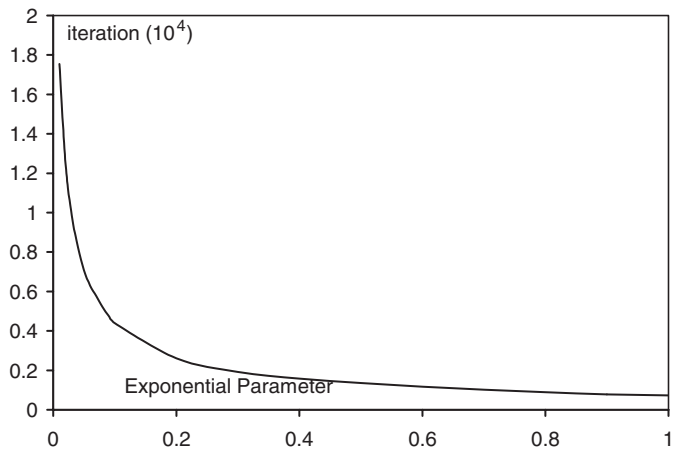

Figure 9. Effect of exponential parameter on convergence.

decreases, and vice versa; with the effect-control factor equal to zero, it is assumed that a good local balance is already reached and no adjustment is needed. With this mechanism, the proposed method takes the advantages from both the conformal mapping and the orthogonal mapping while eliminating the disadvantages of them. It is shown that this method can improve the smoothness greatly with a little sacrifices of the orthogonality, but sometimes the improvements are not sufficient.

In the second modified RL system, the contribution factor is introduced to confine the vicious cycle of mesh overlapping and distortions. It is constructed based on the distance from the grid point to its neighbours. The farther the neighbour is, the larger the contribution factor is, and vice versa. The exponential parameter α controls the effectiveness of the contribution factor. The larger α is, the more effective the contribution factors are, and the smoother the

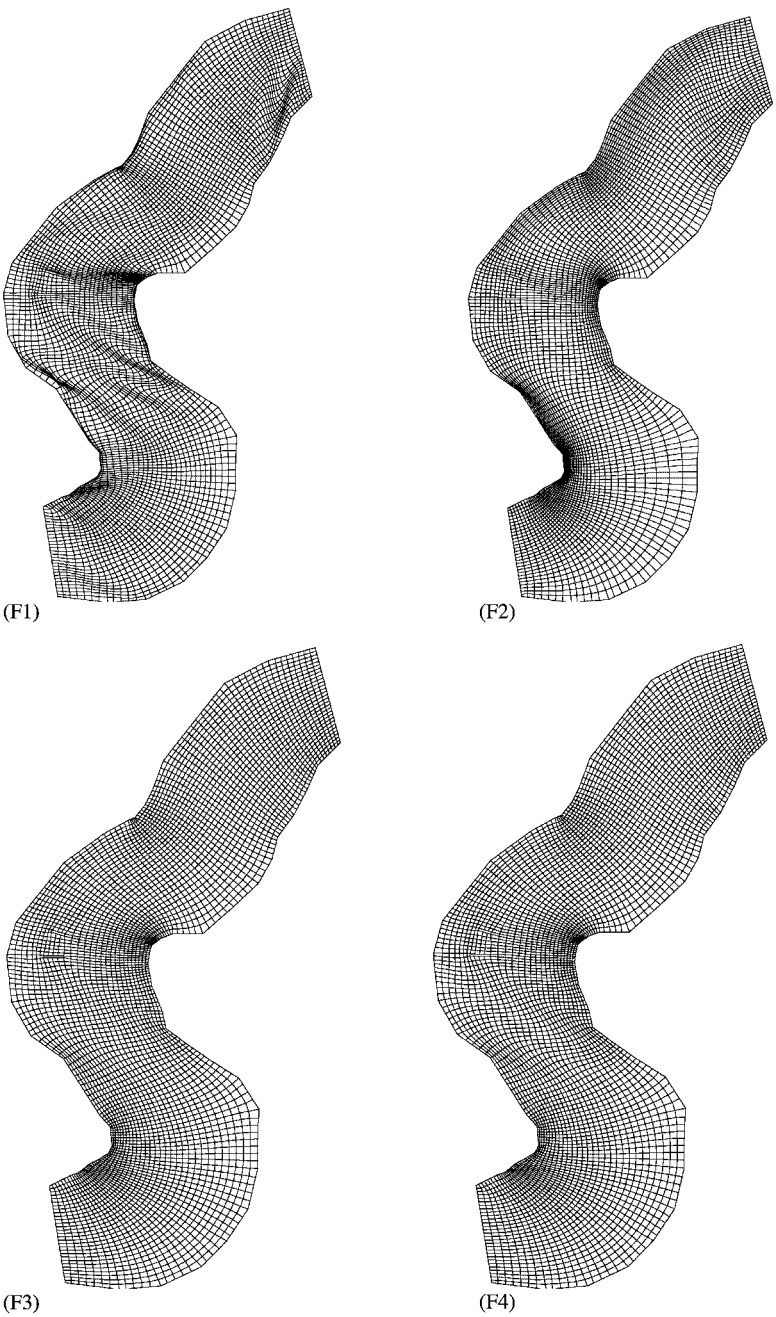

Figure 10. Meshes in domain F with the Dirichlet conditions in all boundaries: (F1) the RL system; (F2) the RL with smoothness control functions; (F3) the RL with contribution factors, $\alpha = 0.3$; and (F4) the hybrid RL system, $\alpha = 0.2$ and $r_C = 1.0$.

Table V. Evaluation of meshes for natural river.

Domain	Case	Size	ADO	MDO	AAR	MAR	α	r_C
F	F1	159×30	1.04	7.72	9.47	32356.00	0.0	0.0
	F2	159×30	0.22	2.69	1.71	8.10	0.0	0.0
	F3	159×30	1.46	6.24	1.44	3.55	0.3	0.0
	F4	159×30	1.50	6.38	1.43	3.49	0.2	1.0

mesh will be. It is found that the parameter α can also speed up the convergence greatly (see Figure 8). Tested examples show that the second method can resolve the mesh distortion and overlapping problem effectively at a little cost of the orthogonality.

The hybrid RL system combines the above two methods. It is flexible to generate a mesh with a mixed effect of both methods. It is shown that the RL system with contribution factors is the best for generating a smooth mesh, and the hybrid RL is in the middle.

The sensitivity analysis shows that the modified RL systems are insensitive to the initial conditions (see, for example, domain C). Therefore, they are stable and can be applied in more general cases. An application to a natural river shows that the modified RL systems are capable of producing quality meshes for practical problems when the original RL fails.

ACKNOWLEDGEMENTS

This work is a result of research sponsored by the USDA Agriculture Research Service under Specific Research Agreement No. 58-6408-2-0062 (monitored by the USDA-ARS National Sedimentation Laboratory) and The University of Mississippi.

REFERENCES

1. Hung TK, Brown TD. An implicit finite-difference method for solving the Navier–Stokes equations using orthogonal curvilinear coordinates. *Journal of Computational Physics* 1977; **23**:343–363.
2. Pope SB. The calculation of turbulent recirculating flows in general orthogonal coordinates. *Journal of Computational Physics* 1978; **26**:197–217.
3. Mobley CD, Stewart RJ. On the numerical generation of boundary-fitted orthogonal curvilinear coordinate systems. *Journal of Computational Physics* 1980; **34**:124–135.
4. Thomas PD, Middlecoff JF. Direct control of the grid point distribution in meshes generated by elliptic systems. *AIAA Journal* 1980; **18**:652–657.
5. Ryskin G, Leal LG. Orthogonal mapping. *Journal of Computational Physics* 1983; **50**:71–100.
6. Tamamidis P, Assanis DN. Generation of orthogonal grids with control of spacing. *Journal of Computational Physics* 1991; **94**:437–453.
7. Allievi A, Calisal SM. Application of Bubnov–Galerkin formulation to orthogonal grid generation. *Journal of Computational Physics* 1992; **98**:163–173.
8. Kang IS, Leal LG. Orthogonal grid generation in a 2D domain via the boundary integral technique. *Journal of Computational Physics* 1992; **102**:78–87.
9. Oh HJ, Kang IS. A non-iterative scheme for orthogonal grid generation with control function and specified boundary correspondence on three sides. *Journal of Computational Physics* 1994; **112**:138–148.
10. Duraiswami R, Prosperetti A. Orthogonal mapping in two dimensions. *Journal of Computational Physics* 1992; **98**: 254–268.
11. Eça L. 2D orthogonal grid generation with boundary point distribution control. *Journal of Computational Physics* 1996; **125**:440–453.
12. Akcelik V, Jaramaz B, Ghattas O. Nearly orthogonal two-dimensional grid generation with aspect ratio control. *Journal of Computational Physics* 2001; **171**:805–821.
13. Tsay TK, Hsu FS. Numerical grid generation of an irregular region. *International Journal for Numerical Methods in Engineering* 1997; **40**:343–356.

14. Knupp P, Steinberg S. *Fundamentals of Grid Generation.* CRC Press: Boca Raton, 1994.
15. Beale SB. A finite volume method for numerical grid generation. *International Journal for Numerical Methods in Fluids* 1999; **30**:523–540.
16. Thompson JF, Thames FC, Mastin CW. TOMCAT—a code for numerical generation of boundary-fitted curvilinear coordinate system on fields containing any number of arbitrary two-dimensional bodies. *Journal of Computational Physics* 1977; **24**:274–302.
17. Thompson JF, Warsi ZUA, Mastin CW. *Numerical Grid Generation*: *Foundation and Application.* North-Holland: New York, 1985.
18. Thompson JF. A reflection on grid generation in the 90s: trends, needs, and influences. *5th International Conference on Grid Generation in CFS*, Mississippi State University, 1996.

